Theoretical and Applied Climatology (2021) 145:955–965
https://doi.org/10.1007/s00704-021-03659-0

ORIGINAL PAPER

Variability of extreme precipitation events in the Northeastern Argentine region

Vanina S. Aliaga[1] · María Cintia Piccolo[1,2]

Received: 11 February 2020 / Accepted: 13 May 2021 / Published online: 9 June 2021

Abstract

The Northeastern Argentine (NEA) region is one of the most productive and vulnerable to climate risk due to frequent extreme precipitation events (EPE). The present study aims to identify and explain the spatiotemporal distribution of precipitation in the NEA region to assess its heterogeneity. A cluster analysis from Ward's hierarchical method was applied using observational precipitation collected at meteorological stations during 1959–2018. The elbow method and a nonhierarchical analysis of K-means were also useful to define the correct number of clusters. The three groups obtained responded to an east-west precipitation gradient that generated a zonal atmospheric circulation, and the positive anomalies mostly coincided with El Niño-Southern Oscillation (ENSO) events. Although they had similar seasonal rainfall and annual amplitudes, each subregion presented its specific variability at different temporal scales. Positive anomalies were more significant in the east of the NEA region, which is reflected in the displacement of isohyets in the last decades. Our results suggest that almost the entire NEA region is highly vulnerable to EPE, but with higher intensity and frequency in the center and east. Due to the agricultural and ecological importance of this region and the socioeconomic effects of EPE, studies with more detailed scales than the regional ones are necessary.

1 Introduction

Climate change impacts are multiscale, with both positive and negative consequences that affect the sustainable development of regions (Nan et al. 2011). In addition, climate variability may lead to variation in the frequency of extreme events that disturb ecosystems and food production and adversely impact human settlements (García and Pedraza 2008). Southeastern South America presents substantial departures from the mean climate at different timescales leading to frequent extreme precipitation events (EPE; Magrin et al. 2014). Flood-related disasters are the most frequent type of hazard in South America (57%) and represent the main cause of economic losses of the remaining natural catastrophes (WMO 2014). Therefore, EPE is the most devastating and costly factor, and several observational studies have found that these events have increased in frequency and severity. Recurring wet events during 1970–2005 generated floods with severe consequences on productive systems and forced population displacements (Lovino et al. 2018).

The Northeastern Argentine (NEA) region, usually called the Mesopotamia, is the richest in biodiversity than any other region in Argentina. This area extends over important hydrological basins with abundant rivers and streams. Furthermore, it is a highly productive region where the main economic activities are logging and its related industries, such as wood and paper. The NEA region is sensitive to climate variability with potential consequences on water resources and very varied agricultural activities. The principal rivers present low coasts, and increased precipitation causes severe floods in urban and rural areas due to high discharges (Lovino et al. 2014; Magrin et al. 2014). Two of the major floods in this region occurred in 1983 and 2003. In both cases, more than 100,000 people had to be evacuated, and there were economic losses in the millions (Krepper and Zucarelli 2010; WMO 2014). Intermittent floods from 2014 to the present have also caused severe damage in the region.

Most of the studies related to EPE in the NEA region have been conducted at the South American level. Responses to

✉ Vanina S. Aliaga
valiaga@iado-conicet.gob.ar; aliagavanina@gmail.com

[1] Instituto Argentino de Oceanografía (IADO – CONICET), Florida 8000, Complejo CCT CONICET Bahia Blanca, Edificio E1, B8000BFW, Bahía Blanca, Argentina

[2] Departamento de Geografía y Turismo, Universidad Nacional del Sur, 12 de Octubre 1198, 4°piso, B8000CTX Bahía Blanca, Argentina

climate variability are generally sought in sea surface temperature anomalies associated with El Niño and La Niña episodes that produce unusual heat and water vapor fluxes from the tropical Pacific Ocean to the atmosphere. There are significant impacts on seasonal and monthly precipitation amounts in numerous regions of South America during the different El Niño-Southern Oscillation (ENSO) phases (Tedeschi et al. 2016). Several studies have related precipitation in southeastern South America to the interannual ENSO timescales, showing increased precipitation and thus leading to higher river flows. However, evidence has also been found that regional decadal variability may be strongly modulated by natural climatic variations (Vera et al. 2010).

The NEA region is described as homogeneous according to climate, resources, and relief. However, in such a large region, significant differences have often been found when considering their climate and variability, thus defining a more detailed zoning (Aliaga et al. 2016; Carvalho et al. 2016; Fazel et al. 2018; Lu et al. 2019). The present study was aimed at evaluating whether there are subregions in the NEA region that have their specific rainfall regime and variability, and thus improve our understanding of EPE using daily and monthly rainfall. These results could be of significance in modeling regional precipitation changes to global and zonal climate variations. They may have practical application in subregional-scale aquatic ecosystem conservation and flood management. In addition, climate change projections and their impact on society and ecosystems have become a vital issue for decision-makers.

2 Materials and methods

2.1 Precipitation data set

In the present paper, the NEA region is considered a heterogeneous area in terms of relief, climate, and natural resources, delimited by −24.29° <lat <− 32.14°, −53.70° <long <− 62.70° (Fig. 1). The NEA region has an area of approximately 350,000 km^2 and contains several Argentine provinces (Fig. 1). The historical data set was obtained from 48 meteorological stations (Fig. 1) provided by the National Institute of Agricultural Technology (INTA, Argentina) and the National Meteorological Service (SMN, Argentina). The analyzed period covered from 1959 to 2018, expressed in daily and monthly rainfall data.

2.2 Methods

2.2.1 Cluster analysis

The goal of clustering is the statistical classification of individual objects into groups. A hierarchical grouping method was considered due to its extensive use to define groups that have high internal homogeneity (Aliaga et al. 2017). Ward's cluster analysis was applied to generate groups considering precipitation, in which N objects are divided into several clusters so that the objects in the same cluster are similar to each other. The process then finds at each stage those clusters whose merger gives the minimum increase in the total within-group error sum of squares. The Euclidean distance was used as a dissimilarity measure, which—according to Oliveira et al. (2017)—is appropriate for climatic data regionalization in South America. As a variable for the cluster examination, precipitation from each of the stations was selected, resulting in three climatologically homogeneous subregions.

Hierarchical clustering analysis was applied to identify the appropriate number of clusters through the elbow method (Zhang et al. 2016). This method examines the percentage of variance explained as a function of the number of clusters. The grouping number is plotted linearly to identify the moment at which changes in distance are no longer significant. At some point, the marginal gain drops dramatically and will give an angle in the graph. The correct "k" number of clusters is chosen at this point, hence the *elbow* criterion. Once the number of groups has been defined, a nonhierarchical analysis—in this case, K-means—is applied to determine the composition of each cluster. K-means is one of the most popular clustering methods based on partitioning. It is a very simple and fast algorithm for cluster head selection. The combination of these methodologies has been tested positively by several authors (Bholowalia and Kumar 2014; Zambelli 2016; Syakur et al. 2018).

2.2.2 Climate interpolation data

Interpolation is a geostatistical exploration technique to estimate unknown values of any geographic point data: elevation, rainfall, temperature, etc. Interpolation calculates values for cells in a raster from a limited number of sample data points (Samanta et al. 2012). In this case, the kriging method based on statistical models including autocorrelation was applied. Kriging aims to develop a better linear impartial estimate for an unknown location. The projected values are weighted linear combinations of the available data because the mean error is 0 (Menafoglio et al. 2013). Ordinary kriging was chosen assuming no trend in the area data, with a regular spherical size of 0.01. This technique has shown results with a better fit to the climatological data analysis (Zhang et al. 2015; Aalto et al. 2016; Karki et al. 2016).

2.2.3 Precipitation variability and trend

Once the rainfall zoning was defined, the Fourier transform was applied to the data of each cluster. The purpose of applying a mathematical transformation to a series is to obtain useful information of the series that is hidden in its frequency contents, which is called the series spectrum and demonstrates

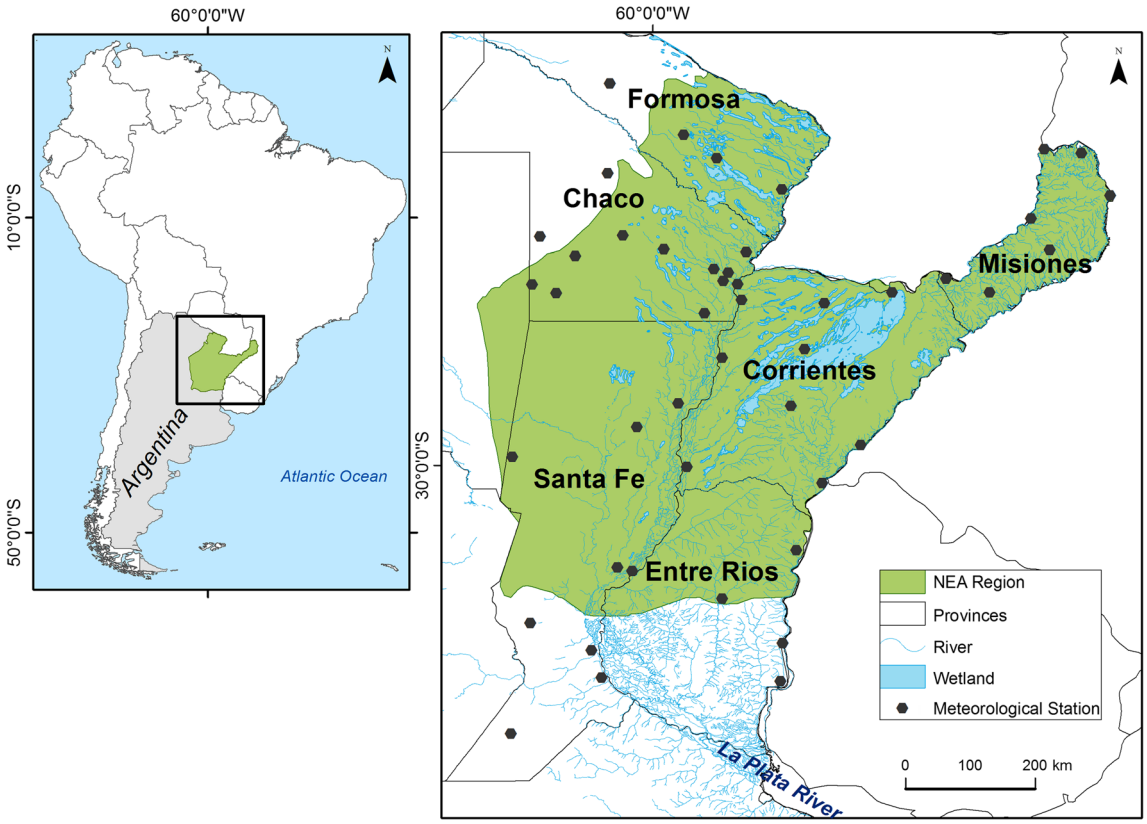

Fig. 1 The NEA region (Argentina) in the southeast of South America; its main rivers, wetlands, and meteorological stations were chosen considering record length and completeness

the frequencies existing in the data series. The algorithm called fast Fourier transform (FFT), obtained following the methodology by Daneshmand et al. (2015), was used in this case.

The Standardized Precipitation Index (SPI) was designed to quantify the precipitation deficit for several timescales, reflecting the impact on the availability of different water resources. Thus, it was chosen and applied to the rainfall data series to identify dry and wet events. It is a helpful indicator to assess the impact on water resources and several activities (Yagoub et al. 2017). SPI has been widely applied for analysis at different spatial and temporal scales and recommended as the most appropriate for South American regions (Orlowsky and Seneviratne 2013; Paulo et al. 2016; Penalba and Rivera 2016). SPI was calculated considering 3-, 6-, and 12-month timescales, which allowed representing short- and long-term events, respectively (monthly, seasonal, and annual scales). To highlight the frequency and intensity of rainfall events, only values ≥ 1.0 were analyzed, including moderate (1.0–1.49), severe (1.5–1.9), and extreme (>2.0) intensities. The possibility of calculating SPI at various timescales allows temporary flexibility in precipitation conditions concerning water supply. These timescales reflect the effects of EPE on different water resources. Shorter term timescales (weeks to months) are used to characterize meteorological conditions relevant to agricultural activities since soil moisture has a relatively fast response to precipitation anomalies. Longer term timescales (from seasons to years) are used to monitor hydrological settings significant for water supply management since groundwater, streamflow, and reservoir storage reflect longer term precipitation anomalies (Sirdas and Sen 2003; OMM 2012).

The spatiotemporal displacement of isohyets at a decadal scale was performed. The trend was also studied using the average anomalies of each group during the study period. Rainfall variability was related to ENSO events through the Oceanic Niño Index (ONI) (https://origin.cpc.ncep.noaa.gov/products/analysis_monitoring/ensostuff/ONI_v5.php), developed by the National Oceanic and Atmospheric Administration (NOAA, USA), which allows identifying warm (El Niño) and cold (La Niña) events in the Tropical Pacific Ocean (http://www.cpc.ncep.noaa.gov/). Warm events occur with the development of a positive SST anomaly (> +0.5 °C), whereas cold events are defined by the occurrence of a negative anomaly (< −0.5 °C).

3 Results and discussions

3.1 Rainfall distribution and zoning

The combination of two cluster analyses and the elbow method determined that the optimum number of clusters for the

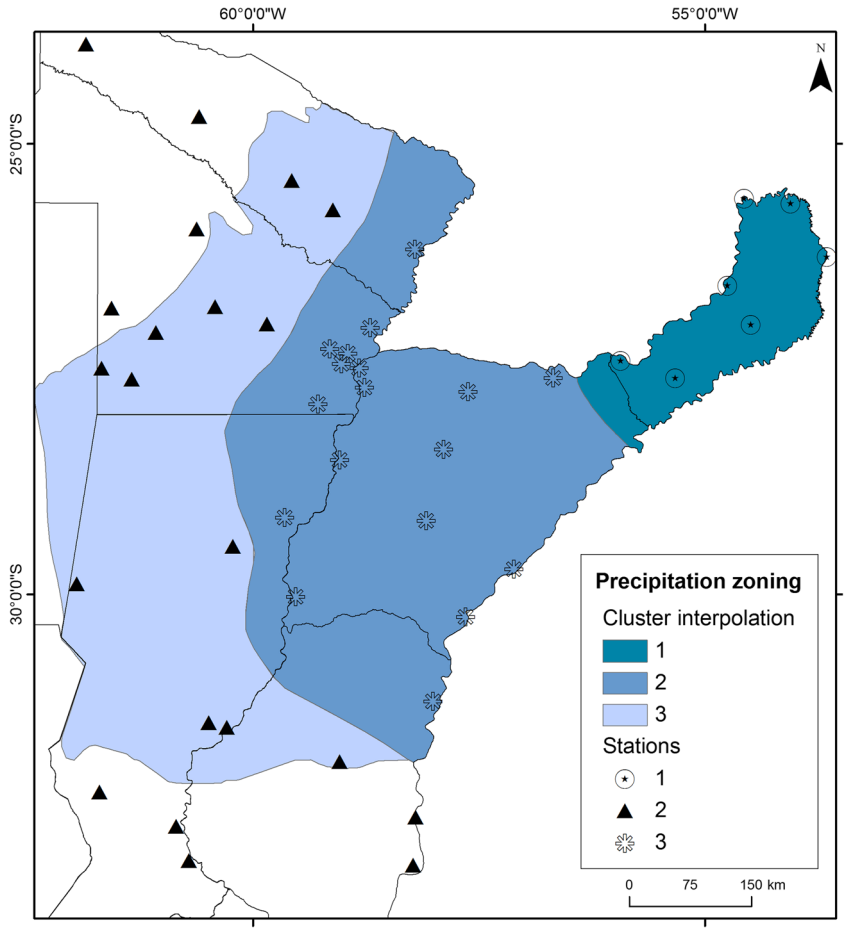

Fig. 2 Precipitation zoning through the interpolation of the three clusters (represented by meteorological stations) in the NEA region (study period 1959–2018)

NEA region was three (Fig. 2). Hereinafter, we will refer to the three clusters as C1, C2, and C3. These clusters represent the daily and monthly precipitation from the 48 meteorological stations located in the NEA region. Cluster arrangement indicated the transition from a very wet climate in the northeast to a moderately humid climate toward the east (Fig. 3). The zoning showed a gradient, in which precipitation decreased from east to west. The average rainfall decreased from 1840 to 1010 mm/year (C1 to C3; Fig. 3).

Seasonal rainfall was observed in all clusters with the highest rainfall in spring and autumn (southern hemisphere). The three subregions registered the minimum annual rainfall in the winter months (July–August). In C1, the maximum precipitation was recorded in the spring months (October),

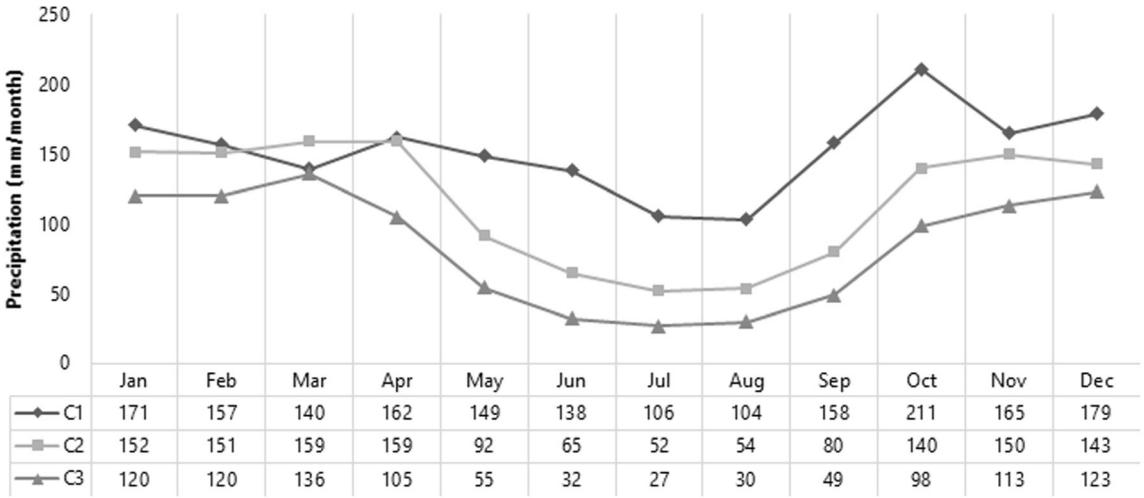

	Jan	Feb	Mar	Apr	May	Jun	Jul	Aug	Sep	Oct	Nov	Dec
C1	171	157	140	162	149	138	106	104	158	211	165	179
C2	152	151	159	159	92	65	52	54	80	140	150	143
C3	120	120	136	105	55	32	27	30	49	98	113	123

Fig. 3 Annual distribution of average monthly precipitation in C1, C2, and C3 of the NEA region (study period 1959–2018)

whereas in C2 and C3 (Fig. 3), it occurs in the autumn months (March–April). Although rainfall decreases toward the west, annual amplitudes were similar in the three subregions, approximately 107 mm/year. The progressive precipitation decreases between the clusters respond to the dominant atmospheric circulation, characterized by high relative humidity due to the entrance of wet air masses entering the continent from the South Atlantic Anticyclone. These air masses generally come from the east and northeast, and they discharge moisture in the form of precipitation throughout the region, decreasing to the west.

3.2 Subregional precipitation variability

The FFT analysis showed different signals in each cluster. Some of them respond to an interdecadal variation, such as 15 years in C2. Within the interannual frequencies, those of 8, 4, and 2 years were identified (Fig. 4). The annual signal is the most intense in all groups, although, in C2, it has a higher domain with respect to the other frequencies. The 6-, 4-, and 2-month signals were also present throughout the NEA region. Data transformation allows observing that, although there are similar seasonality and annual amplitude of rainfall in the three clusters (Fig. 3), the yearly seasonal frequency is noticeably higher toward the west (Fig. 4). The density spectra show that C1 has a low seasonal rainfall regime, whereas, in C2 and C3, the precipitation seasonality is well defined.

Tropical-oceanic atmosphere oscillations affect rainfall variability at low latitudes; in the NEA region, it is influenced by the South Atlantic Ocean anticyclone. The South Atlantic convergence zone has a quasi-stationary character and variability over a wide range of timescales, contributing to the annual variation of rainfall in the southern hemisphere, as observed in each cluster (Gilliland and Keim 2018; Kayano et al. 2019). The interannual and seasonal frequencies could be related to the Madden Julian Oscillation (MJO; Bridgman and Oliver 2006). Alvarez et al. (2016) determined the regional influence of the MJO swing in South America, along with its marked seasonal variations. In December–February (summer), when the South American monsoon system was active, there was a higher precipitation frequency. In March–May (autumn), it was similar but attenuated in the extra-tropics. In September–November (spring), higher rainfall was also observed, coinciding with those shown in Fig. 3. These signals are generated primarily through the propagation of the Rossby Wave energy produced by the anomalous heating region associated with MJO (Alvarez et al. 2016).

Values of ≥ 1.0 were analyzed to highlight the frequency and intensity of SPI wet categories in the NEA region. Table 1 shows the number of events per year on three timescales (3, 6, and 12 months) for each cluster. The complete analysis allows observing the relationship between the frequency of events and the timescale used to calculate SPI. The frequency

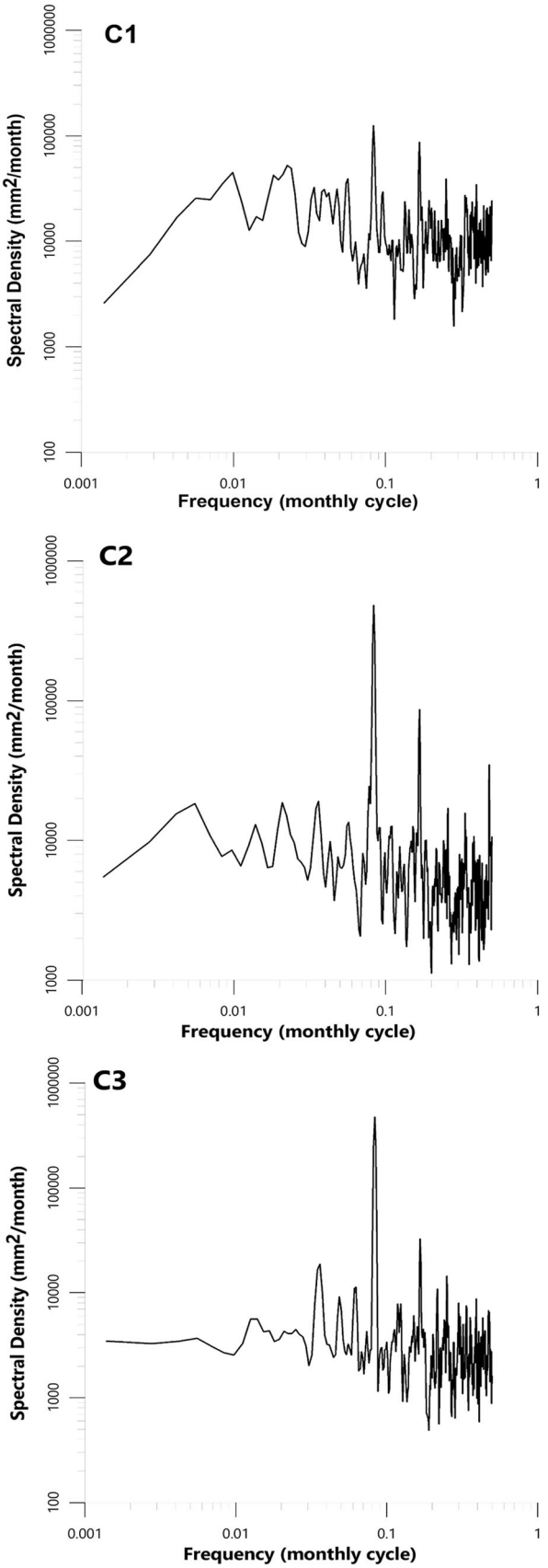

Fig. 4 Spectral density of monthly precipitation in C1, C2, and C3 by fast Fourier transform (study period 1959–2018)

Table 1 Number and intensity of EPE according to SPI per year on three timescales (3, 6, and 12 months). Summary of total of events and maximum intensity registered in each cluster and category (study period 1959–2018)

	Cluster1 - SPI 3				Cluster1 - SPI 6				Cluster1 - SPI 12				Cluster 2-SPI 3				Cluster 2-SPI 6				Cluster 2-SPI 12				Cluster 3-SPI 3				Cluster 3-SPI 6				Cluster 3-SPI 12			
Year	Mod	Sev	Ext	Σ	Mod	Sev	Ext	Σ	Mod	Sev	Ext	Σ	Mod	Sev	Ext	Σ	Mod	Sev	Ext	Σ	Mod	Sev	Ext	Σ	Mod	Sev	Ext	Σ	Mod	Sev	Ext	Σ	Mod	Sev	Ext	Σ
1959				-				-				-			1	1				1				-	1	2		3	2	2	1	5				-
1960	1	1		2				-				-	1	1		2	1	1		2		1		1	2			2	1			1				-
1963	1			1				-				-				-				-				-				-				-				-
1965	2	1		3	1	1		2	1			1	1	2		3	1	1		2				-		1		1	1			1				-
1966	1			1	1	1		2	1*			1	1	1	1	3		1	1*	2	2	2*	1	5		2	1	3	1	2	1	4	1	1		2
1967				-				-				-	1			1	1			1				-			1	1	1	1	1	3				-
1968				-				-				-	2			2				-				-	1			1				-				-
1969				-				-				-	1			1				-				-				-				-				-
1970				-				-				-		1		1				-				-				-				-				-
1971	1			1				-				-				-				-				-	1			1	1			1				-
1972	1	1*	1	3	2	1*	1	4				-	2	1		3	2	1		3				-	1	2	1	4	1	1		2				-
1973				-		1		1	2*	1		3	2	1*		3	2*	1*		3	2	1*		3	1	2	1	4	2	3	1	6		2	1*	3
1974				-				-				-				-				-	1			1				-				-	1			1
1975			1*	1		2*	2	4	3*	3		6				-				-				-				-	1			1				-
1977				-				-				-	1			1				-				-				-				-				-
1978				-				-				-	1			1	1			1				-	3	2		5	3	1		4	4			4
1979	1			1				-				-	1			1				-				-				-				-				-
1980				-				-				-				-				-				-	1	1		2	1			1				-
1981				-				-				-				-				-				-	1	2		3	3	2		5	3	2		5
1982	2	1		3	1	1		2				-	2	2	1	5	2	1	1	4				-	1	1		2	1*			1				-
1983	1	2	1*	4	2		1*	3	1	1	1*	3	1	2		3	2*	2		4	1	3*	1	5	1		1	2	2			2	2			2
1984				-				-	1	1	1	3	1			1	1			1				-	2	2		4	2			2	2*			2
1985	1			1	1			1				-	1	2		3	2	1*		3	1			1	2	1		3	1			1				-
1986	1	1		2	1*			1				-	1	2	1*	4		2	2*	4	1*		1	2	3*	3	1	7	2	2*	2	6	1*	1	1	3
1987	2			2	1	1		2	1			1	1			1				-	1		1*	2	1			1	1			1	1	1*		2
1989	1*			1				-				-				-				-				-				-				-				-
1990	1	2*	1	4	1	2*	1	4	1	1*		2	2*	2		4	3*			3	1	1		2		1		1	1			1	1			1
1991				-	1	1		2	1	1*		2	1			1	2			2				-		2	1	3	3	1	1	5	3*	1		4
1992	1			1	1			1				-	1*			1	1*			1	1			1	1	1		2				-	2			2
1993				-				-				-	1			1				-	1			1	2	1		3	2			2				-
1994	1			1				-				-				-				-				-				-				-				-
1995				-	1			1				-	1			1				-				-				-				-				-
1996	2		1	3	1			1				-	2			2				-				-				-				-				-
1997	2*			2	1	2*		3	3	2*		5	1	2		3	1	1		2				-	1			1				-				-
1998	2	2*	2	6	1	1*		2	2	3*	2*	7		1	1*	2		1	1*	2	1	1	1*	3	1	2	1	4	2	1	1*	4	1	1*		2
1999				-				-	1			1				-				-	1			1				-				-				-
2000	1			1	2			2				-				-				-				-	3	2	1	6	2	2	1	5		1		1
2001	1	1		2	2	1		3	1*			1	1			1				-				-	1	1		2	2			2	1	1	1	3
2002	2	2		4	2	1		3	1*			1	2	2	1	5	1*	2	1	4	1*	1	1	3	2	1		3	2	2	1	5	1*		1	2
2003		2		2	1*			1	1*			1	1			1	1	1*		2	2		1*	3	2			2	3	2*		5	1	1*	1	3
2004				-				-				-	1			1				-				-				-				-				-
2005	1			1				-				-	1			1				-				-	1			1	2			2				-
2006				-				-				-				-				-				-		1		1				-				-
2007	3			3	1*			1	1*			1	1			1				-				-	1	1*		2	2*	1	1	4	1*	2*		3
2009	1	2	1	4	1	1		2				-		1	1	2	1	1		2				-	1			1	1			1				-
2010	1			1	2	1*		3	1*	1		2		1	1	2		1	1*	2	1*	1		2	1	1		2	2*	1		3	1			1
2011				-				-				-				-				-				-				-				-				-
2012	1			1				-				-	1		1	2	1			1				-	2		1	3	1	2		3				-
2013				-	1			1				-				-	2			2				-	1			1	1			1				-
2014	1	2	2*	5	2		1*	3	1	1	1*	3				-				-				-				-	1			1				-
2015	2	1	2	5	2*		1	3	2	2*	1	5	3	1		4	2		1	3	1			1	1			1				-				-
2016			1*	1	1	2	1*	4	1	1*		2	2	1*		3	2	2	1	5	3*	2*		5	2			2	1			1				-
2017	2*	1		3	1			1	1			1	2	1	1	4	3	2		5	3	2		5				-				-	1			1
2018				-	2			2	1*			1				-				-	2*			2				-				-				-
Sum	41	22	13	76	37	20	8	65	29	18	6	53	45	27	10	82	35	23	9	67	27	15	7	49	45	35	10	90	55	26	11	92	28	14	5	47
Máx value				3.0				3.2				2.9				3.0				3.1				3.0				2.8				2.5				2.4

*At least one event lasted for 3 or more months

decreases as the timescale increases. Therefore, the highest number of events was recorded on the 3-month scale in all NEA subregions. However, the 3-month events were more frequent in C3. This scale reflects short- and medium-term humidity conditions and provides a seasonal estimate of precipitation. In central agricultural regions, such as the NEA region, a 3-month SPI could be more effective in highlighting the existence of humidity conditions than the Palmer index (OMM 2012). Comparing the 3-month SPI with more extended timescales allows identifying wet events in the middle of a long-term drought, avoiding misinterpretations. Information derived from a 6-month SPI reflects the effects on river flows and abnormal storage levels, which are markedly higher in C3 (Table 1). The 12-month SPI shows a higher frequency in C1 and is generally linked to effects on river channels, reservoir levels, and even groundwater levels.

Moderate events are predominant in all groups, although they decrease as the timescale increases. In the east of the NEA region, extreme events are more notable than in the rest of the region. To the west, C2 and C3 have a high number of total events, represented by a higher number of mainly moderate and severe events (Table 1). In C1, the highest frequencies were recorded in the years 1973, 1975, 1983, 1990, 1998, 2014, and 2015. They coincide with the most extended events in 1975, 1983, 1998, and 2014. The highest number of wet events was recorded in 1998, whereas the period of the highest intensity was in 1975. In C2, most events were recorded in 1966, 1983, and 2014–2016, coinciding in this case with the longest duration events. Finally, in C3, the highest number of wet events was recorded in 1972, 1973, 1978, 1981, 1986, 1991, 2001–2003, and 2007, coinciding in 1991 and 2001–2007 with those of the longest duration.

In terms of intensities, in C1, the most extreme SPI values were recorded in all 3-, 6-, and 12-month timescales, with values of 3.0, 3.2, and 2.9, respectively. As mentioned, in C1 the event with the highest value was recorded in 1975, with a value of 3.03 (Fig. 5). There were also other considerably high values in 1972, 1983, and 1998, as well as the continuity of EPE in 2014–2016. In C2, the most intense extreme events were recorded in 1959, 1986, 1998, and 2010. The latter marked the maximum value of SPI: 2.95. Finally, in C3, they were recorded in 1972, 1991, and 2000, with the highest value of 2.84 in 1991. These EPE periods are usually related to the intense activity in the convergence zone of the South Atlantic Ocean (Carvalho et al. 2004), which could explain these intensities in the north of the NEA region (Cerne and Vera 2011).

The analysis of precipitation anomalies allows identifying that C1 presents the most significant anomalies, both positive and negative (Fig. 6). The variability of the anomalies decreases toward the west; in C3, it oscillates in ±200 mm/year.

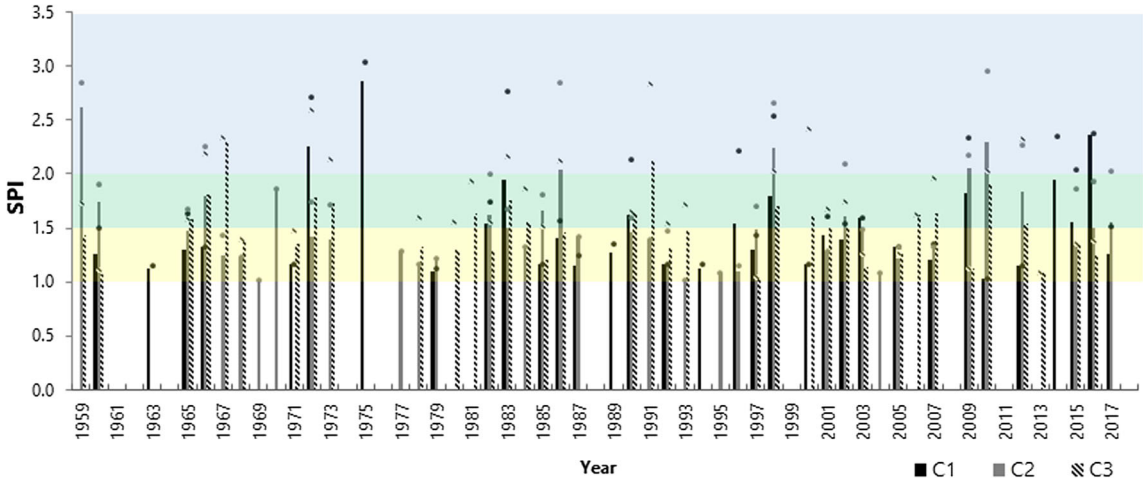

Fig. 5 Averages (bars) and maximum (dots) of EPE per year according to the 3-month SPI in C1, C2, and C3 of the NEA region. Moderate (yellow), severe (green), and extreme (blue) intensities (study period 1959–2018)

The most severe negative anomalies occurred in 1977 and 1994 in C1, whereas the positive ones were identified in 1982 and 2013–2015. During the rest of the study period, several similarities in the anomalies are observed between C1 and C2. The maximum positive anomalies that coincide with the floods of 1983 and 1985 stand out as those of the most significant damage in the study area (WMO 2014). It is noticeable that at the subregional level, all have a positive trend in terms of annual anomalies; however, in C1, it is considerably higher (Fig. 6).

The isohyets displacement (Fig. 7) exposes the extreme positive anomalies (1982, 2013–2015). Every three decades, the last one experiences an increase in precipitation represented by the movement of its isohyets (1981–1990 and 2011–2018). This could suggest that, in the previous decade (1950s), there was also a period of extreme rainfall, following the decadal frequency observed for 60 years. Although rainfall data are not available, strong El Niño events were recorded in 1957 and 1958 (NOAA-http://www.cpc.ncep.noaa.gov). The isohyets displacement in C1 and C2 agrees with the positive trend of precipitation anomalies (Fig. 6), as well as with the evidence obtained in studies showing a positive trend in terms of precipitation increase in the NEA region and other regions in Argentina (Doyle et al. 2012; Barros et al. 2015). As shown by the spatial distribution of isohyets and anomalies, this positive trend in precipitation is not similar throughout the region. This increase in rainfall in most of subtropical Argentina (C1 and C2) since 1960 has favored agricultural yields and the extension of agricultural land, but also the most frequent heavy rains and the consequent flooding of rural and urban areas. Floods have also been encouraged by changes in land use (Barros et al. 2015; Carril et al. 2016). Many of the positive trends in the precipitation series were statistically significant at 10%, and in some cases even at 5%, confidence level. In addition, there is paleoclimate evidence that the wetting trend that began in 1960 has been unprecedented in at least 250 years (Piovano et al. 2002).

C1 shows significant similarities between the intensity of ENSO-El Niño events (ONI ≥0.5) and monthly rainfall (Fig. 8). In particular, highlights reached in 1966, 1972, 1983,

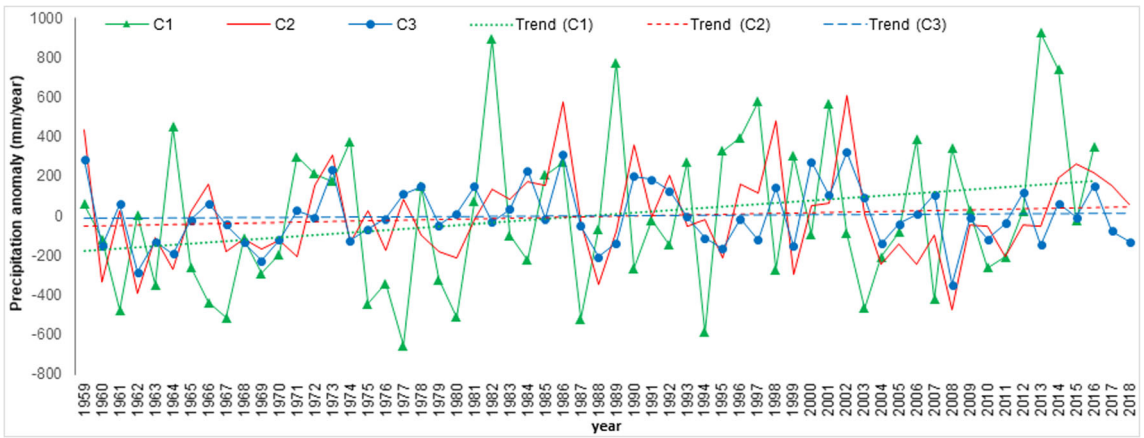

Fig. 6 Annual rainfall anomaly (solid lines) and lineal trend (intermittent lines) in C1, C2, and C3 of the NEA region (study period 1959–2018)

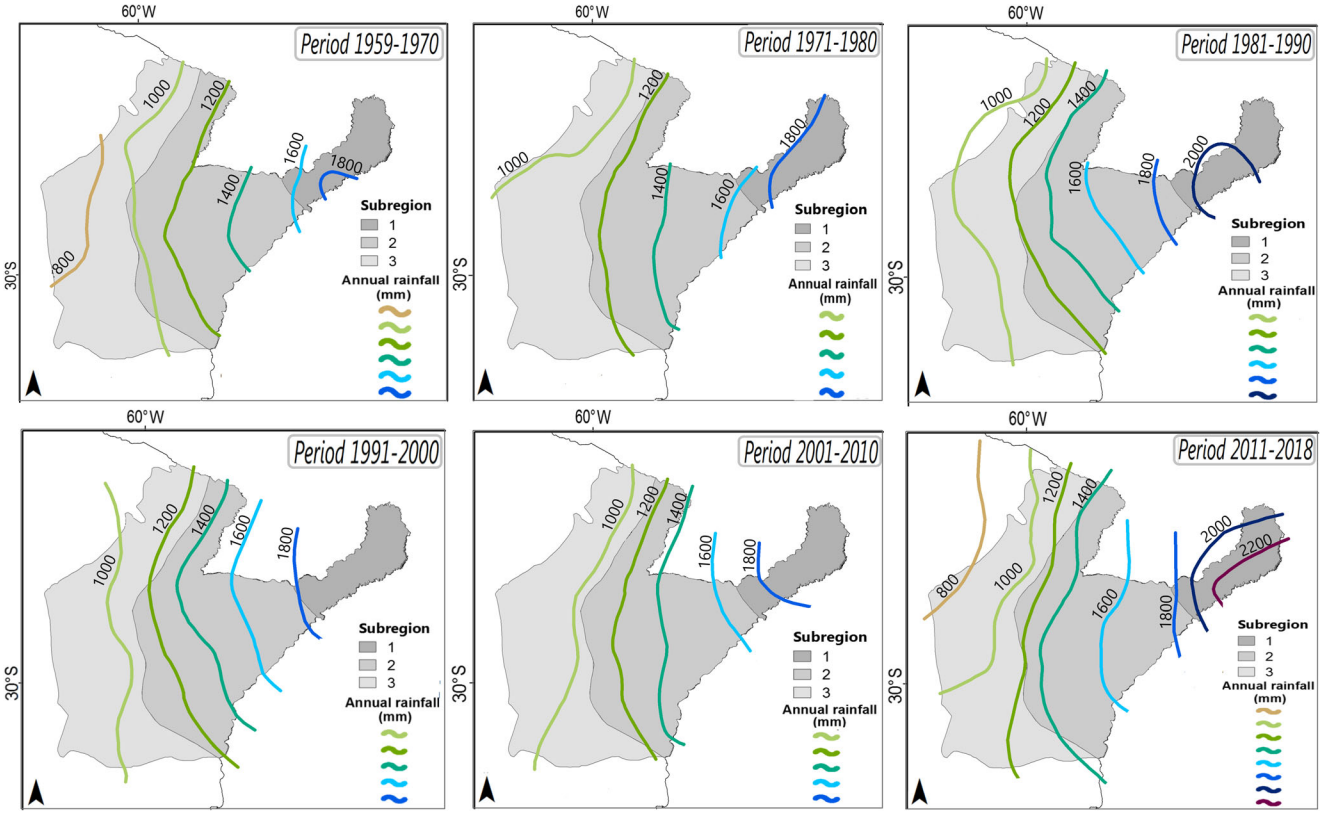

Fig. 7 Decadal spatial displacement of isohyets (from 800 to 2200 mm/year) throughout the three rainfall subregions of the NEA region (study period 1959–2018)

1997–1998, 2010, and 2015–2016. Only in 1975, there was an EPE that is not visibly influenced by ENSO. In the center of the NEA region, C2 presents coincidences with C1, except in 1997 and 2015, when there was no notable increase in rainfall above average. In C3, to the mentioned periods, coincidences in 1964, 1978, and 1992 are added. Therefore, C3 shows a higher frequency of extreme rainfall coincidences with El Niño events, according to ONI. This agrees with the responses found to the increased precipitation in the NEA region. Since 1960, they can be explained by a positive association between precipitations in ENSO indices (Barros et al. 2015). The NEA region has a maximum positive correlation of annual rainfall with the southward displacement of the South Atlantic Anticyclone that increases the wet advection of the Atlantic Ocean (Sun et al. 2017; Gilliland and Keim 2018). Given the dependence of monthly and seasonal precipitation amounts on the frequency of EPE, it is reasonable to expect to be modulated by ENSO at some preferred locations. As the most dramatic social and economic impacts of climate variability are due to the associated variability of extreme events, it is worth detailing the association between ENSO and extreme rainfall events (Tedeschi et al. 2016).

Anomalies and extreme events are not the only cause of flooding. In cases such as those of 1987, 1990, or 1999, anomalies were extraordinary, but there were no massive floods. It has been shown that the incidence and severity of floods are increasing. This is attributed to the fact that since the 1960s there have been at least three significant changes that may have affected the hydrometeorology of the region: changes in land use, mainly deforestation, which increases runoff levels; hydroelectric development, which regulates the flow rates; and increased seasonal rainfall.

4 Conclusions

The present paper assesses the heterogeneity of precipitation in the Northeastern Argentine region. Precipitation observations in this region in the period 1959–2018 show that (1) three homogeneous precipitation subregions (C1, C2, and C3) were identified; (2) C1 presented a higher rainfall seasonality than C2 and C3; (3) according to SPI, 3- and 6-month timescale events were more frequent in C3, and 12-month timescale events were more frequent in C1; (4) in the last decade, there was a displacement of isohyets, especially in C1, coinciding with the highest positive trend in the region.

The combination of agglomeration methods allowed obtaining an appropriate number of clusters that represent the precipitation subregions. The clusters show an east-west spatial gradient (2000 to 800 mm/year). The annual amplitude is similar in the three clusters, but in C1, the maximum rainfall

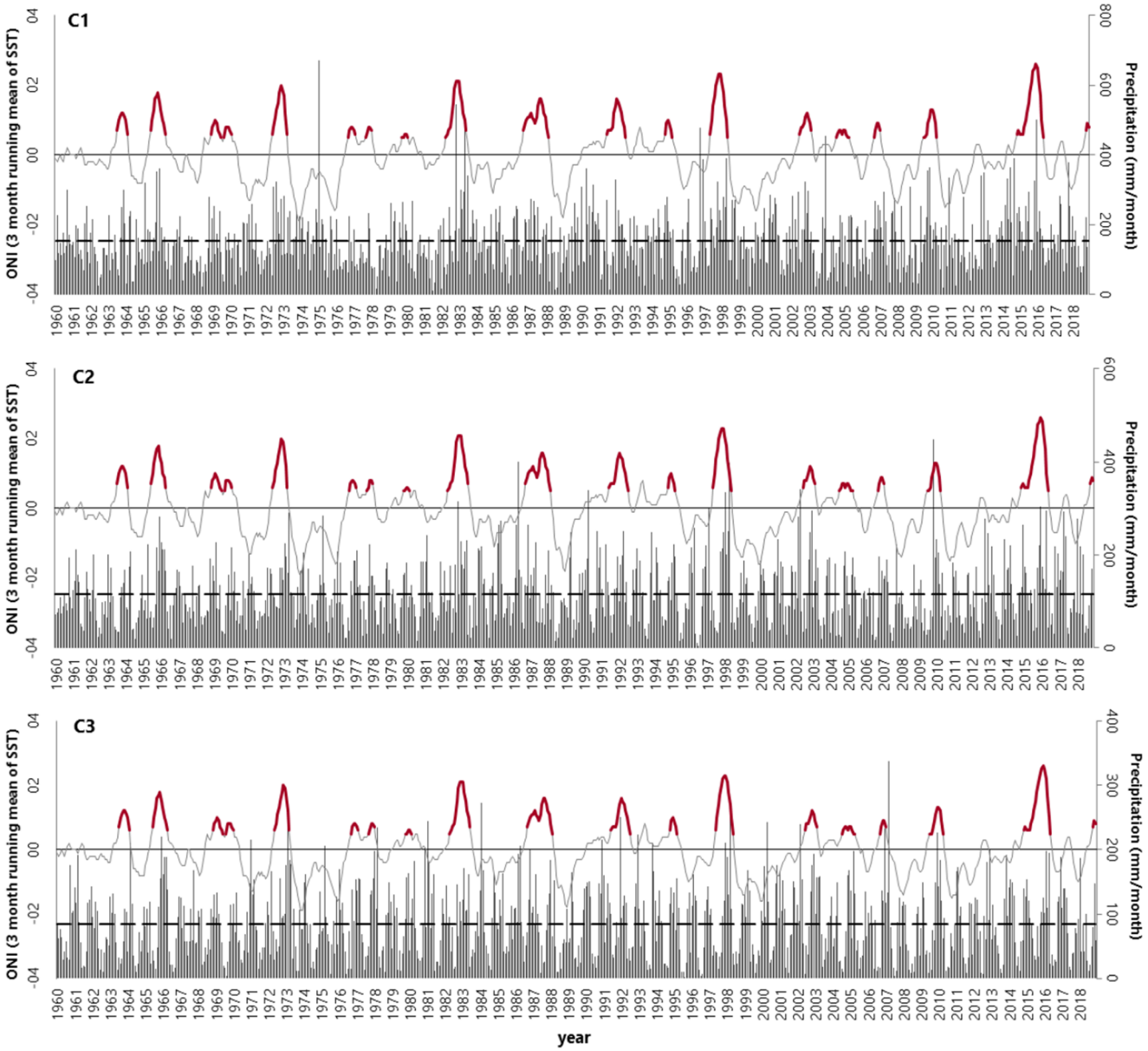

Fig. 8 Specific monthly precipitation (gray bars), monthly average precipitation (intermittent line), and ONI intensity (gray line) in the three clusters of the NEA region. El Niño events are indicated by red lines (study period 1959–2018)

is registered in spring and C2 and C3 in autumn. According to SPI, the frequency of events decreases with the scale of analysis used. In each subregion, moderate events are the most frequent. The EPE scales reflect the range of their effects. In C3, the 3- and 6-month events represent short- and medium-term effects on moisture conditions, provide a seasonal estimate of precipitation in agricultural regions, and reflect effects on river flows and abnormal storage levels. The 12-month SPI shows a higher frequency in C1 and is generally linked to effects on river channels, reservoir levels, and even groundwater levels. The index allowed classifying the periods in which the most significant floods were recorded in the study area (1983, 2003, 1973–1975, and 2014–2016).

The anomaly variability made it possible to identify significant differences between the clusters. Their intensity decreases in the east-west direction. C1 showed the highest positive anomalies in the last 60 years. Although there are coincidences in the periods of positive anomalies in most of the critical wet events (e.g., 2002–2003, 2015–2016), one of the most critical floods in 1983 was only reflected in C1. In agreement with other authors, the analysis of rainfall with ONI showed that ENSO events have a leading influence on the study area and that the intensity and impact of these phenomena vary from one subregion to another (a higher frequency of matches was recorded in C3). Many positive anomalies respond to ENSO events, but they do not explain all recorded

floods or EPE, so there must be other phenomena that cause these anomalies. Considering the different subregional responses, it is essential to conduct studies at the subregional level in terms of the effects of zonal phenomena. The present paper could help in this regard and focus efforts on the efficient development of resources in the NEA region. Due to the damage already being caused by extreme rains, the first and most urgent adaptation required is to strengthen early warning systems and contingency planning to deal with climatic extremes.

Acknowledgements The authors would like to thank the National Meteorological Service (SMN, Argentina) and the National Institute of Agricultural Technology (INTA, Argentina) for supplying the information analyzed in this work. This study was supported by the Inter-American Institute for Global Change Research (IAI) CRN3038 (under US NSF Award GEO-1128040), the Consejo Nacional de Investigaciones Cientificas y Tecnicas (CONICET, Argentina), and the Universidad Nacional del Sur.

Author contribution All authors contributed to the study's conception and design. Material preparation, data collection, and analysis were performed by Vanina S. Aliaga. The first draft of the manuscript was written by Vanina S. Aliaga, and all authors commented on previous versions of the manuscript. All authors read and approved the final manuscript.

Funding This study was supported by the Consejo Nacional de Investigaciones Cientificas y Tecnicas (CONICET) and the Inter-American Institute for Global Change Research (IAI).

Availability of data and material Not applicable.

Code availability Not applicable.

Declarations

Ethics approval We wish to declare that all ethical practices have been followed in relation to the development, writing, and publication of the article. We declare that no animal experiments have been conducted in this investigation, as well as no experiments with human beings. We understand that the corresponding author is the sole contact for the Editorial process (including Editorial Manager and direct communications with the office). She is responsible for communicating with the other authors about progress, submissions of revisions, and final approval of proofs. We confirm that we have provided a current, correct email address, which is accessible by the corresponding author and which has been configured to accept email from (valiaga@iado-conicet.gob.ar – aliagavanina@gmail.com).

Consent to participate Informed consent was obtained from all participants included in this study to the submission of the manuscript to the journal.

Consent for publication The authors consent regarding publishing their data and details within the article "Variability of extreme precipitation events in the Northeast Region of Argentina" in the *TAAC* journal. Signed by all authors as follows: Dr. Vanina S. Aliaga; Dr. Maria Cintia Piccolo.

Conflict of interest The authors declare no competing interests.

References

Aalto J, Pirinen P, Jylhä K (2016) New gridded daily climatology of Finland: permutation-based uncertainty estimates and temporal trends in climate. JGR-Atmos 121:3807–3823. https://doi.org/10.1002/2015JD024651

Aliaga VS, Ferrelli F, Alberdi-Algarañaz ED, Bohn VY, Piccolo MC (2016) Distribution and variability of precipitation in the Pampas, Argentina. Cuad Investig Geogr 42:261–280. https://doi.org/10.18172/cig.2867

Aliaga VS, Ferrelli F, Piccolo MC (2017) Regionalization of climate over the Argentine Pampas. Int J Climatol 37:1237–1247. https://doi.org/10.1002/joc.5079

Alvarez MS, Vera CS, Kiladis GN, Liebmann B (2016) Influence of the Madden Julian oscillation on precipitation and surface air temperature in South America. Clim Dyn 46:245–262. https://doi.org/10.1007/s00382-015-2581-6

Barros VR, Boninsegna JA, Camilloni IA, Chidiak M, Magrín GO, Rusticucci M (2015) Climate change in Argentina: trends, projections, impacts and adaptation. WIREs Clim Change 6:151–169. https://doi.org/10.1002/wcc.316

Bholowalia P, Kumar A (2014) EBK-means: a clustering technique based on elbow method and k-means in WSN. Int J Comput Appl 105(9): 17-24. https://doi.org/10.5120/18405-9674. https://www.ijcaonline.org/archives/volume105/number9/18405-9674

Bridgman HA, Oliver JE (2006) The global climate system: patterns, processes, and teleconnections. Cambridge University Press, Cambridge

Carril AF, Cavalcanti IF, Menendez CG, Sörensson A, López-Franca N, Rivera JA, Da Rocha RP (2016) Extreme events in the La Plata basin: a retrospective analysis of what we have learned during CLARIS-LPB project. Clim Res 68:95–116. https://doi.org/10.3354/cr01374

Carvalho LMV, Jones C, Liebmann B (2004) The South Atlantic Convergence Zone: intensity, form, persistence, and relationships with intraseasonal to interannual activity and extreme rainfall. J Clim 17:88–108

Carvalho MJ, Melo-Gonçalves P, Teixeira JC, Rocha A (2016) Regionalization of Europe based on a K-means cluster analysis of the climate change of temperatures and precipitation. Phys Chem Earth A/B/C 94:22–28. https://doi.org/10.1016/j.pce.2016.05.001

Cerne SB, Vera CS (2011) Influence of the intraseasonal variability on heat waves in subtropical South America. Clim Dyn 36:2265–2277. https://doi.org/10.1007/s00382-010-0812-4

Daneshmand H, Tavousi T, Khosravi M, Tavakoli S (2015) Modeling minimum temperature using adaptive neuro-fuzzy inference system based on spectral analysis of climate indices: a case study in Iran. J Saudi Soc Agric Sci 14:33–40. https://doi.org/10.1016/j.jssas.2013.06.001

Doyle ME, Saurral RI, Barros VR (2012) Trends in the distributions of aggregated monthly precipitation over the La Plata Basin. Int J Climatol 32:2149–2162. https://doi.org/10.1002/joc.2429

Fazel N, Berndtsson R, Uvo CB, Madani K, Kløve B (2018) Regionalization of precipitation characteristics in Iran's Lake Urmia basin. Theor Appl Climatol 132:363–373. https://doi.org/10.1007/s00704-017-2090-0

García NO, Pedraza RA (2008) Daily rainfall variability over northeastern Argentina in the La Plata River basin. Ann N Y Acad Sci 1146(1):303–319. https://doi.org/10.1196/annals.1446.011

Gilliland JM, Keim BD (2018) Position of the South Atlantic anticyclone and its impact on surface conditions across Brazil. J Appl Meteorol Climatol 57:535–553. https://doi.org/10.1175/JAMC-D-17-0178.1

Kayano MT, Andreoli RV, De Souza RA (2019) Pacific and Atlantic multidecadal variability relations to the El Niño events and their

effects on the South American rainfall. Int J Climatol 2019:1–18. https://doi.org/10.1002/joc.6326

Krepper CM, Zucarelli GV (2010) Climatology of water excesses and shortages in the La Plata Basin. Theor Appl Climatol 102:13–27. https://doi.org/10.1007/s00704-009-0234-6

Lovino M, García NO, Baethgen W (2014) Spatiotemporal analysis of extreme precipitation events in the northeast region of Argentina (NEA). J Hydrol: Reg Stud 2:140–158. https://doi.org/10.1016/j.ejrh.2014.09.001

Lovino MA, Müller OV, Müller GV, Sgroi LC, Baethgen WE (2018) Interannual-to-multidecadal hydroclimate variability and its sectoral impacts in northeastern Argentina. Hydrol Earth Syst Sci 22:3155–3174. https://doi.org/10.5194/hess-22-3155-2018

Lu Y, Jiang S, Ren L, Zhang L, Wang M, Liu R, Wei L (2019) Spatial and temporal variability in precipitation concentration over mainland China, 1961–2017. Water 11:881. https://doi.org/10.3390/w11050881

Magrin GO, Marengo JA, Boulanger JP, Buckeridge MS, Castellanos E, Poveda G, Scarano FR, Vicuña S (2014). Central and South America, in: Climate change: impacts, adaptation, and vulnerability. Part B: Regional Aspects. Contribution of Working Group II to the Fifth Assessment Report of the Intergovernmental Panel on Climate Change, edited by: Barros VR, Field CB, Dokken DJ, Mastrandrea MD, Mach KJ, Bilir TE, Chatterjee M, Ebi KL, Estrada YO, Genova RC, Girma B, Kissel ES, Levy AN, MacCracken S, Mastrandrea PR, White LL. Cambridge University Press, Cambridge, United Kingdom and New York, NY, USA, 1499–1566

Menafoglio A, Secchi P, Dalla RM (2013) A universal kriging predictor for spatially dependent functional data of a Hilbert space. Electron J Stat 7:2209–2240. https://doi.org/10.1214/13-EJS843

Nan Y, Bao-hui M, Chun-Kun L (2011) Impact analysis of climate change on water resources. Procedia Eng 24:643–648. https://doi.org/10.1016/j.proeng.2011.11.2710

Oliveira PT, Silva CS, Lima KC (2017) Climatology and trend analysis of extreme precipitation in subregions of Northeast Brazil. Theor Appl Climatol *130*(1-2):77–90. https://doi.org/10.1007/s00704-016-1865-z

Organización Meteorológica Mundial (2012) Guía del usuario sobre el Índice normalizado de precipitación (OMM-N° 1090) Svoboda M, Hayes N, Wood D. Ginebra

Orlowsky B, Seneviratne SI (2013) Elusive drought: uncertainty in observed trends and short-and long-term CMIP5 projections. Hydrol Earth Syst Sci 17:1765–1781. https://doi.org/10.3929/ethz-b-000073994

Paulo A, Martins D, Pereira LS (2016) Influence of precipitation changes on the SPI and related drought severity. An analysis using long-term data series. Water Resour Manag 30:5737–5757. https://doi.org/10.1007/s11269-016-1388-5

Penalba OC, Rivera JA (2016) Precipitation response to El Niño/La Niña events in Southern South America-emphasis in regional drought occurrences. Adv Geosci 42:1–14. https://doi.org/10.5194/adgeo-42-1-2016

Piovano EL, Ariztegui D, Moreira SD (2002) Recent environmental changes in Laguna Mar Chiquita (central Argentina): a sedimentary model for a highly variable saline lake. Sedimentology 49:1371–1384. https://doi.org/10.1046/j.1365-3091.2002.00503.x

Samanta S, Pal DK, Lohar D (2012) Interpolation of climate variables and temperature modeling. Theor Appl Climatol 107:35–45. https://doi.org/10.1007/s00704-011-0455-3

Sirdas S, Sen Z (2003) Spatio-temporal drought analysis in the Trakya region, Turkey. Hydrol Sci J 48:809–820. https://doi.org/10.1623/hysj.48.5.809.51458

Sun C, Kucharski F, Li J, Jin FF, Kang IS, Ding R (2017) Western tropical Pacific multidecadal variability forced by the Atlantic multidecadal oscillation. Nat Commun 8:1–10. https://doi.org/10.1038/ncomms15998

Syakur MA, Khotimah BK, Rochman EMS, Satoto BD (2018) Integration k-means clustering method and elbow method for identification of the best customer profile cluster. In IOP Conf Ser: Mater Sci Eng 336:012017. https://doi.org/10.1088/1757-899X/336/1/012017

Tedeschi RG, Grimm AM, Cavalcanti IF (2016) Influence of central and east ENSO on precipitation and its extreme events in South America during austral autumn and winter. Int J Climatol 36:4797–4814. https://doi.org/10.1002/joc.4670

Vera C, Barangeb M, Dubec OP, Goddardd L, Griggse D, Kobyshevaf N, Odadag E, Pareyh S, Polovinai J, Povedaj G, Seguink B, Trenberthl K (2010) Needs assessment for climate information on decadal timescales and longer. Proc EnvironSci 1:275–286. https://doi.org/10.1016/j.proenv.2010.09.017

World Meteorological Organization (2014) Atlas of mortality and economic losses from weather, climate and water extremes (1970-2012). World Meteorological Organization. WMO-No. 1123. Geneva 2, Switzerland ISBN 978-92-63-11123-4

Yagoub YE, Li Z, Musa OS, Anjum MN, Wang F, Bo Z (2017) Detection of drought cycles pattern in two countries (Sudan and South Sudan) by using Standardized Precipitation Index SPI. Am J Environ Eng 7:93–105. https://doi.org/10.5923/j.ajee.20170704.03

Zambelli AE (2016) A data-driven approach to estimating the number of clusters in hierarchical clustering. F1000Research 5. https://doi.org/10.12688/f1000research.10103.1

Zhang F, Zhong S, Yang Z, Sun C, Huang Q (2015) Spatial estimation of mean annual precipitation (1951–2012) in Mainland China based on collaborative kriging interpolation. Geo-Informatics in Resource Management and Sustainable Ecosystem. Springer, Berlin Heidelberg, pp 663–672. https://doi.org/10.1007/978-3-662-49155-3_69

Zhang Y, Moges S, Block P (2016) Optimal cluster analysis for objective regionalization of seasonal precipitation in regions of high spatial–temporal variability: application to Western Ethiopia. J Clim 29:3697–3717. https://doi.org/10.1175/JCLI-D-15-0582.1

Karki R, Talchabhadel R, Aalto J, Baidya SK (2016) New climatic classification of Nepal. Theoretical and applied climatology, 125(3);799–808